

MODELING OF LONG-CABLE-FED INDUCTION MOTOR DRIVE SYSTEM FOR PREDICTING OVERVOLTAGE TRANSIENTS

L. Wang¹ and J. Jatskevich²

¹*ABB Sweden Inc. Corporate Research, Vasteras, SE-721 78, Sweden*

²*University of British Columbia, Vancouver, BC V6T 1Z4, Canada*

Induction motor drive systems fed with cables are widely used in many industrial and agricultural applications. Accurate prediction of motor terminal overvoltage, caused by impedance mismatch between the long cable and the motor, plays an important role for motor dielectric insulation and optimal design of dv/dt filters. In this paper, modeling methodology for the investigation of long-cable-fed induction motor drive overvoltage is proposed. An improved high-frequency motor equivalent circuit model is developed to represent the motor high-frequency behavior for the time- and frequency-domain analyses. A high-frequency cable model based on improved high-order multiple- π sections is proposed. The proposed methodology is verified on an experimental 2.2kW ABB motor drive benchmark system. The motor overvoltage transients predicted by the proposed model is in excellent agreement with the experimental results.

High-frequency modeling, induction motor drives, long cable, overvoltage transients.

Adjustable speed drives are undergoing significant changes with the successful application of novel power semiconductor devices. The rise and fall switching times of newer devices have been decreasing in order to reduce switching losses and increase the overall efficiency. However, very fast switching times coupled with the long cables can cause voltage reflection at the motor terminals due to cable-motor surge impedance mismatch [1]–[2]. In some cases, the motor terminal overvoltage can reach two times of the dc bus voltage [3]–[4], which may seriously harm the motors' dielectric insulation leading to subsequent failures [5]–[6]. Therefore, accurate modeling of the cable-fed motor-drive systems in the high-frequency range is crucial for predicting the motor terminal overvoltage and designing mitigation filters [7]–[10].

A typical system composed of a motor-drive feeding an induction machine through a cable is shown in Fig. 1. In order to facilitate the high frequency cable and motor modeling and characterization, two modes of operations, common mode (CM) and differential mode (DM) [11] are usually considered. The CM is formed as a two-port network between the parallel-connected three phases and ground wire. The DM is regarded as a two-port network between two parallel-connected phases and the third phase of the cable motor system.

Numerous high-frequency motor models have been proposed in the literature for overvoltage and electro-magnetic interference (EMI) analysis [12–18]. In [17], an efficient high frequency motor model is proposed for the studies of both DM and CM behaviors in time- and frequency-domain. In [18], a universal

induction machine model with low-to-high frequency-response characteristics is proposed.

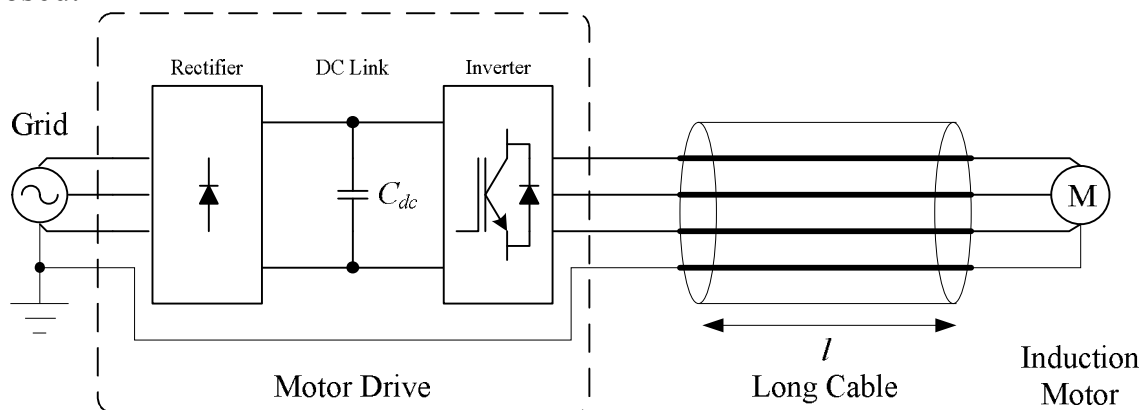


Fig. 1. Typical motor-drive system with connecting cable

This model is quite sophisticated as the DM, CM and bearing models are all integrated into one three-phase motor equivalent circuit. Modeling of long cables for analysis of motor voltage reflection phenomena has been studied as well [7, 8, 9], [19–23]. Various cable models were proposed including conventional multiple- π section model with 2nd-order per-section [7, 8], lossless [9], [19], lossy [20, 21, 22], and frequency-dependent [15], [23] transmission line models. This paper presents an improved motor model [24] that captures the high-frequency DM and CM impedance characteristics, as well as the cable model which includes both the skin and proximity effects and the dielectric losses for the high frequency range.

High-Frequency Induction Motor Modeling: Accurate modeling of induction motors in high-frequency range plays an important role in overvoltage and EMI problems [12–18]. The high-frequency motor model used in this paper is based on per-phase equivalent circuit proposed in [17]. The circuit diagram of the motor per-phase high-frequency model is illustrated in Fig. 2 (a). This circuit provides relatively simple model structure. However, the parameters R_{ad} and C_{ad} in Fig. 2 (a) are very difficult to express using analytical formulas [17]. Instead, trials and adjustments of R_{ad} and C_{ad} are usually required with the help of frequency-domain simulations to achieve satisfactory results [17]. In this paper, an improved high-frequency model is proposed as shown in Fig. 2 (b). The proposed circuit uses similar model structure and parameterization procedure as in [17]. However, a series R_t , L_t and C_t branch is introduced (see Fig. 2 (b)) to replace the R_{ad} and C_{ad} branch (see Fig. 2 (a)) without sacrificing model accuracy [24]. Since this new series branch has its own resonance, analytical calculation of parameters R_t , L_t and C_t can be carried out in a more straightforward way from the measured impedances [24].

The equivalent-circuit depicted in Fig. 2(b) and its parameters also have physical meaning and significance. In particular, R_{g1} and C_{g1} represent the parasitic resistance and capacitance between the stator winding and the motor frame; R_{g2} and C_{g2} represent the parasitic resistance and capacitance between the

stator neutral and motor frame; L_d represents the stator winding leakage inductance; R_e represents the high-frequency iron loss of the stator winding; L_t and C_t are introduced to capture the second resonance in the motor impedance characteristic, which may be caused by the skin effect and inter-turn capacitance of the stator windings.

The overall equivalent-circuit model is identified through the DM and CM impedance characteristics of the motor measured in frequency-domain. The detailed DM and CM measurements setup and test procedures have been well documented in the literature, e.g., [17]. The detailed derivations for the branch parameters are not included here due to limited space, whereas interested reader can find more background information in [13], [15], and [24].

Based on the per-phase equivalent circuit Fig. 2 (b), the combined DM motor equivalent circuit is shown in Fig. 3 (a). The high-frequency CM motor equivalent circuit is built by connecting all three phases in parallel. Based on per-phase equivalent circuits of Fig. 2 (b), the resulting CM motor equivalent circuit from phase to ground is shown in Fig. 3 (b). The corresponding parameters are summarized in Table I.

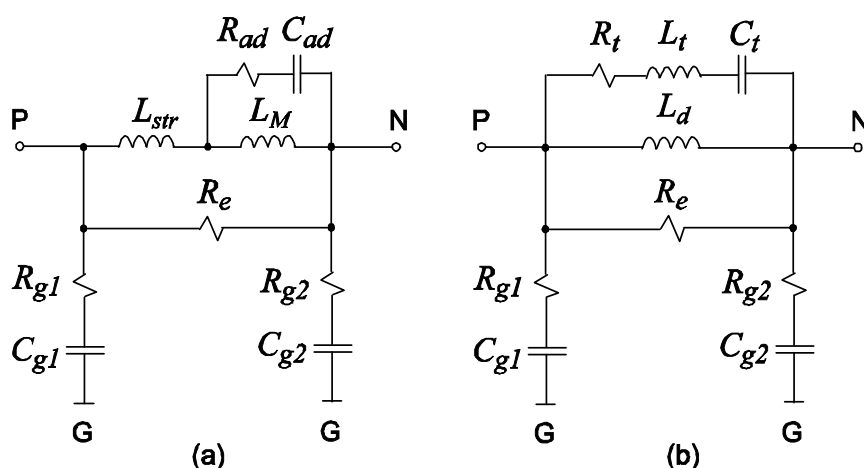


Fig. 2. High frequency per-phase motor equivalent-circuits: (a) model defined in [17]; and (b) proposed model

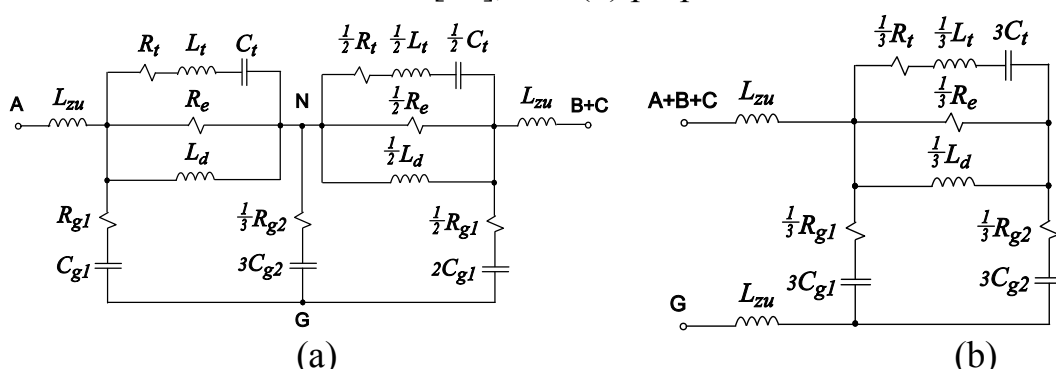


Fig. 3. High-frequency equivalent circuit motor model: (a) for DM assuming phases B and C are connected in parallel; and (b) for CM between the three connected phases and ground

High-Frequency Cable Modeling: Accurate modeling of power cable is also essential for predicting motor terminal overvoltage. Since the overvoltage transient at the motor end may contain oscillations in wide range of frequencies from several hundred Hz to several MHz depending on the cable characteristic and length, the cable model should also include the frequency-dependent phenomena such as skin and proximity effects, dielectric losses, etc. The available methods for modeling cables at this level and extracting parameters include Finite Element Analysis (FEA) [22] or direct impedance measurement [15], [25] in frequency domain using precision impedance analyzers. In this paper, the same impedance analyzer was also used to characterize the cable.

The short circuit (SC) and open circuit (OC) tests in differential mode [22], [25] have been performed upon which the cable parameters were calculated. The resulting per-section equivalent circuit is just a conventional 2nd-order per-section cable model shown in Fig. 4 (a) [7], [8]. The advantage of equivalent circuit of Fig. 4 (a) is of course its simplicity. The parameters for this circuit are typically identified at the resonant frequency of motor terminal overvoltage. However, the resonant frequency itself will also depend on the cable length and may be difficult to predict with good accuracy. An improved cable model was proposed in [15], which can represent the dielectric losses using a higher-order parallel branch as shown in Fig. 4 (b). Further improvements are proposed in this paper in order to include the skin and proximity effects. Such effects are not taken into account with the use of first-order series branch. Therefore, a high-order model is proposed in Fig. 4 (c). This section model combines the parallel branches as proposed in [15] and utilizes higher-order series branches to represent skin and proximity effects. Overall, one additional inductor and capacitor are utilized in the per-section model compared with the classic 2nd-order constant parameter cable model. To identify the parameters of the circuit of Fig. 4 (c), the circuit response is considered in the low- and high-frequency ranges, respectively [24].

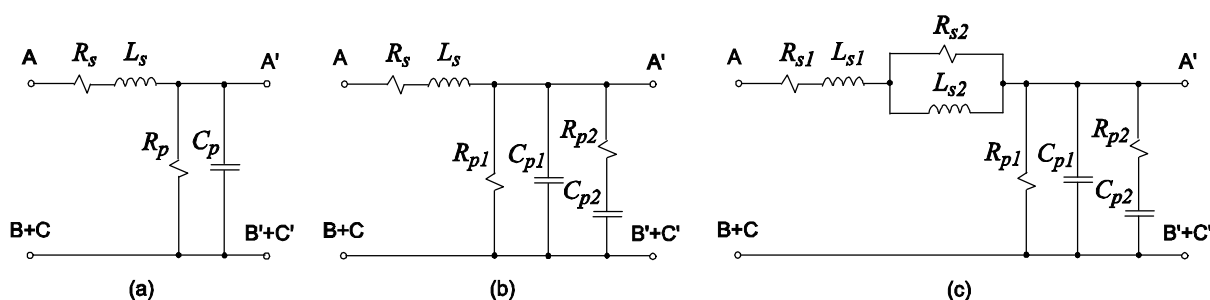


Fig. 4. Per-section DM cable models: (a) conventional; (b) improved model [15]; and (c) proposed model

Experimental Verification: To validate the methodology described in this paper, the experimental tests with long-cable-fed motor drive system have been carried out and are presented in this section. The drive system is ABB 2.2 kW ACS50 type with switching frequency of 16 kHz. The rise and fall times of IGBT switches are on the order of 190 μ s. The power cable is an unshielded, PVC

insulated, 4-core cable with the conductor area of 1.5 mm^2 . The same 4-pole, 2.2 kW, ABB (model number: M2AA100LA) induction machine was used in all tests.

In order to demonstrate the importance of including frequency-dependent effects in cable modeling, two conventional models and the proposed model are have been considered. All considered models use multi- π sections equivalent circuits to approximate the distributed-parameter effects, wherein the length of each cable-section is assumed to be 0.1m. The conventional models use 2nd-order per-section equivalent circuit shown in Fig. 4 (a) with parameters R_s , L_s , R_p and C_p measured at low- high-frequency (1 kHz, Conventional model 1) and high-frequency (0.4 MHz, Conventional model 2), respectively. For consistency, the corresponding parameters are summarized in Table III. The proposed 4th-order per-section cable model has also been used. The model parameters were identified according to the experimental procedure described in [24] and results are summarized in Table II.

To demonstrate the overvoltage phenomena on the considered motor-drive system with a 100m cable, the measured line-to-line voltages at the inverter side and the motor terminal are shown in Fig. 5. As can be seen in this figure, the rectangular pulses generated by the inverter switching produce oscillatory transient and significant overvoltage at the motor terminal. A fragment of Fig. 5 has been magnified and superimposed with the simulated responses produced by the proposed and conventional models as depicted in Fig. 6 (a) and (b), respectively. As can be seen in Fig. 6 (a), the proposed model predicts more accurately both the waveform and the damping than either of the conventional models in Fig. 6 (b). The models are further compared to the experimental results for the 70m and 120m cables, as shown in Fig. 7 and Fig. 8, respectively. It is observed in Figs. 6 (b), 7 (b), and 8 (b) that the conventional models 1 and 2 either over- or under-estimate the overvoltage peaks. Also, since the attenuation and distortion effect due to frequency-dependence are not represented, the shape of the overvoltages predicted by models 1 and 2 are also more square-like. The overall damping of the overvoltage transient predicted by the model 1 is also much longer compared with model 2. This also clearly shows that using the 2nd-order section-model with either low- or high-frequency parameters (see Table III) is not adequate to cover the spectrum of the overvoltage phenomena. At the same time, the proposed model demonstrates good results in predicting the overvoltage peaks, shape, as well as damping as can be clearly seen in Figs. 6(a) – 8(a).

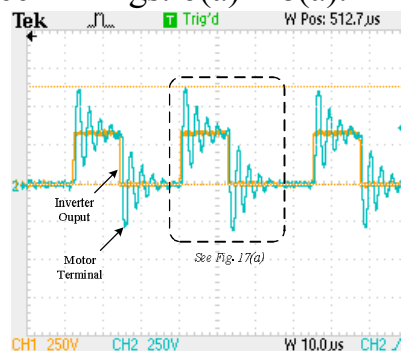


Fig. 5. Measured voltage waveforms at the inverter and motor terminals for 100m cable

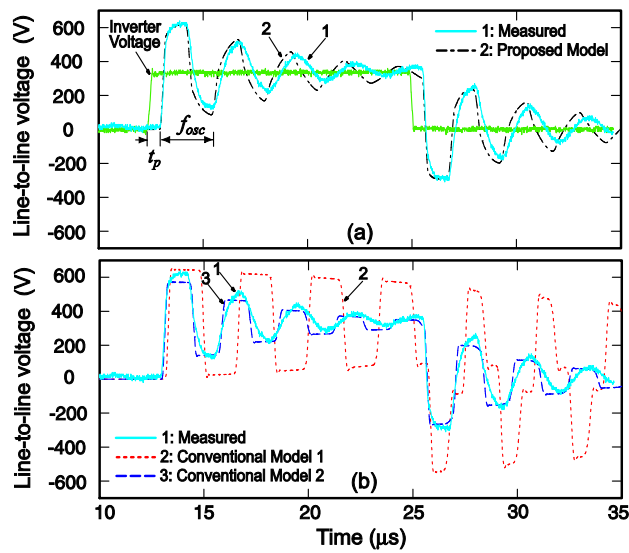


Fig. 6. Measured voltage waveforms at the motor terminals for 100m cable: (a) proposed model; (b) conventional model 1 and 2

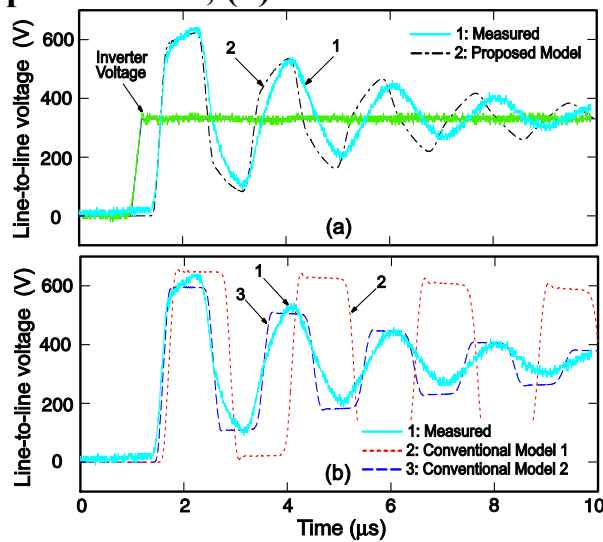


Fig. 7. Measured voltage waveforms at the motor terminals for 70m cable: (a) proposed model (b) conventional models 1 and 2

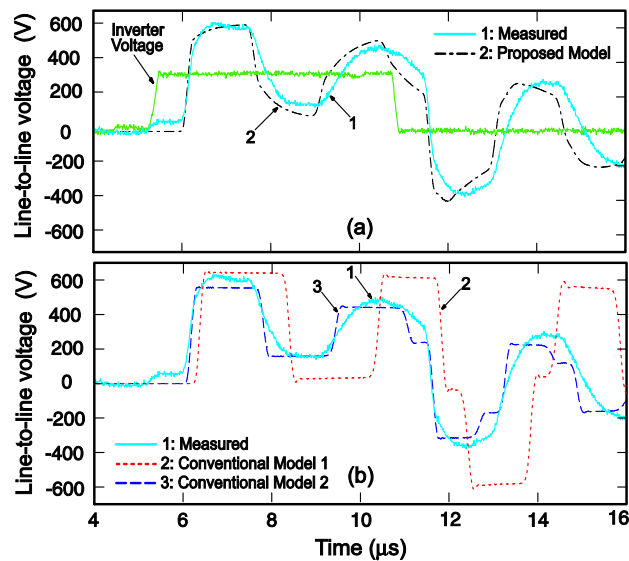


Fig. 8. Measured voltage waveforms at the motor terminals for 120m cable: (a) proposed model (b) conventional model 1 and 2

Conclusions

This paper has proposed a high-frequency modeling methodology for the long-cable-fed motor drive system to predict the overvoltage transients. An improved high-frequency motor model was proposed which accurately represents the high-frequency DM and CM impedance characteristics from hundreds of Hz to tens of MHz. A frequency-dependent cable model is developed which includes the skin- and proximity-effects as well as dielectric losses. The model parameters are easily identified from the measured DM impedance characteristics in a wide frequency range from hundred Hz to ten MHz. The proposed methodology is verified experimentally as well as compared against two conventional modeling techniques. It is shown that the proposed model represents an appreciable improvement in predicting the long-cable-fed motor drive overvoltage transients.

List of References

1. E. Persson, "Transient effects in application of PWM inverters to induction motors," *IEEE Trans. Ind. Appl.*, vol. 28, no. 5, pp. 1095–1101, Sept./Oct. 1992.
2. L. A. Saunders, G. L. Skibinski, S. T. Evon, D. L. Kempkes, "Riding the reflected wave – IGBT drive technology demands new motor and cable considerations," in *Proc. IEEE Petroleum and Chemical Industry Conference 1996*, Philadelphia, PA, Sept. 23–25, 1996, pp. 75–84.
3. R. Kerkman, D. Legate, and G. Skibinski, "Interaction of drive modulation and cable parameters on AC motor transients," *IEEE Trans. Ind. Appl.*, vol. 33, no. 3, May/June 1997, pp. 722–731.
4. S. Amarir, and K. Al-Haddad, "Mathematical analysis and experimental validation of transient over-voltage higher than 2 per unit along industrial ASDM long cables," in *Proc. IEEE Power Electronics Specialists Conference, PESC 2008*, Montreal, QC, Canada, pp. 1846–1851.
5. A. H. Bonnett, "Analysis of the impact of pulse-width modulated inverter voltage waveforms on AC induction motors," *IEEE Trans. Ind. Appl.*, vol. 32, no. 2, Mar./Apr. 1996, pp. 386–392.
6. ABB Technical Guide No. 102: Effects of AC Drives on Motor Insulation – Knocking Down the Standing Wave, ABB Industrial Systems, Inc., New Berlin, WI, USA, 1997.
7. N. Aoki, K. Satoh, A. Nabae, "Damping circuit to suppress motor terminal overvoltage and ringing in PWM inverter-fed AC motor drive systems with long cable leads," *IEEE Trans. Ind. Appl.*, vol. 35, no. 5, Sept./Oct. 1999, pp. 1014–1020.
8. A. Jouanne, D. A. Rendusara, P. N. Enjeti, and J. W. Gray, "Filtering techniques to minimize the effect of long motor leads on PWM inverter-fed AC motor drive systems," *IEEE Trans. Ind. Appl.*, vol. 32, Jul./Aug. 1996, pp. 919–926.

9. S. Lee, and K. Nam, "Overvoltage suppression filter design methods based on voltage reflection theory," *IEEE Trans. Power Electron.*, vol. 19, no. 2, Mar. 2004, pp. 264–271.

10. A. F. Moreira, P. M. Santos, T. A. Lipo, and G. Venkataramanan, "Filter networks for long cable drives and their influence on motor voltage distribution and common-mode currents," *IEEE Trans. Ind. Electron.*, vol. 52, no. 2, pp. 515–522, Apr. 2005.

11. J. D. Irvin, *The Industrial Electronics Handbook*, CRC / IEEE Press, Florida, 1997.

12. E. Zhong, and T. A. Lipo, "Improvements in EMC performance of inverter-fed motor drives," *IEEE Trans. Ind. Appl.*, vol. 31, no. 6, Nov./Dec. 1995, pp. 1247–1256.

13. A. Boglietti and E. Carpaneto, "Induction motor high frequency model," in *Conf. Rec. IEEE IAS Annual Meeting*, Phoenix, AZ, Oct. 1999, pp. 1551–1558.

14. G. Grandi, D. Casadei, and A. Massarini, "High frequency lumped-parameter model for AC motor windings," in *Proc. EPE'97*, vol.2, Trondheim, Norway, 1997, pp. 578–583.

15. A. F. Moreira, T. A. Lipo, G. Venkataramanan, and S. Bernet, "High-frequency modeling for cable and induction motor overvoltage studies in long cable drives," *IEEE Trans. Ind. Appl.*, vol. 38, no. 5, pp. 1297–1306, Sept./Oct. 2002.

16. S. Weber, E. Hoene, S. Guttowski, W. John, and H. Reichl, "Modeling induction machines for EMC-analysis," in *Proc. 35th IEEE Annual Power Electronics Specials Conference*, Aachen, Germany, 2004, pp. 94–98.

17. M. Schinkel, S. Weber, S. Guttowski, W. John, and H. Reichl, "Efficient HF modeling and model parameterization of induction machines for time and frequency domain simulations," in *Proc. IEEE APEC*, Dallas, TX, 2006, pp. 1181–1186.

18. B. Mirafzal, G. Skibinski, R. Tallam, D. Schlegel, and R. Lukaszewski, "Universal induction motor model with low-to-high frequency-response characteristics," *IEEE Trans. Ind. Appl.*, vol. 43, no. 5, Sept./Oct. 2007, pp. 1233–1246.

19. S. Amarir, and K. Al-Haddad, "A modeling technique to analyze the impact of inverter supply voltage and cable length on industrial motor-drives," *IEEE Trans. Power Electron.*, vol. 23, no. 2, pp. 753–762, Mar. 2008.

20. G. Skibinski, D. Leggate, and R. Kerkman, "Cable characteristics and their influence on motor overvoltages," in *Proc. 12th Annual Applied Power Electronics Conference and Exposition*, 1997, vol. 1, pp. 114–121.

21. G. Skibinski, R. Kerkman, D. Leggate, J. Pankau, and D. Schlegel, "Reflected wave modeling techniques for PWM AC motor drives," in *Proc. IEEE APEC'98*, vol.2, Anaheim, CA, Feb. 15–19, 1998, pp. 1021–1029.

22. G. Skibinski, R. Tallam, R. Reese, B. Buchholz, and R. Lukaszewski, "Common-mode and differential-mode analysis of 3 phase cables for PWM AC drives," in *Conf. Rec. IEEE IAS Annual Meeting*, Tampa, FL, Oct. 6, 2006, pp. 880–888.

23. G. Oriti, and A. L. Julian, "Application of the transmission line theory to the frequency domain analysis of the motor voltage stress caused by PWM inverters," Proc. of IEEE IAS Annual Meeting 2004, Seattle, WA, Oct. 2004, pp. 1996–2002.

24. L. Wang, C. N.M. Ho, F. Canales, and J. Jatskevich, "High-Frequency Modeling of the Long-Cable-Fed Induction Motor Drive System Using TLM Approach for Predicting Overvoltage Transients," IEEE Trans. on Power Electronics, Vol. 25, Iss. 10, pp. 2653 – 2664, Oct. 2010.

25. Y. Weens, N. Idir, R. Bausiere, and J. J. Franchaud, "Modeling and simulation of unshielded and shielded energy cables in frequency and time domains," IEEE Trans. Magn., vol. 42, no. 7, Jul. 2006, pp. 1876–1882.

Table I High frequency motor parameters

Parameter	Value	Parameter	Value
R_{g1}	10.57 Ω	C_{g1}	462 pF
R_{g2}	42.94 Ω	C_{g2}	422 pF
R_t	2.9 k Ω	C_t	147 pF
R_e	8.11 k Ω	L_t	43.2 mH
L_{zu}	411 nH	L_d	17.2 mH

Table II The proposed model cable per-meter parameters

Parameter	Value	Parameter	Value
R_{s1}	21 m Ω	L_{s1}	451.8 nH
R_{s2}	271.2 m Ω	L_{s2}	89.32 nH
R_{p1}	22 M Ω	C_{p1}	79.6 pF
R_{p2}	100 k Ω	C_{p2}	34.11 pF

Table III Conventional cable model per-meter parameters

A) At 1kHz

Parameter	Value	Parameter	Value
R_s	21 m Ω	L_s	580 nH
R_p	16.9 M Ω	C_p	114.6 pF

B) At 0.4MHz

Parameter	Value	Parameter	Value
R_s	120 m Ω	L_s	530 nH
R_p	66.2 k Ω	C_p	80.9 pF